ff

GSI

GSI-Preprint-97-05
Januar 1997

WHAT KIND OF RADIOBIOLOGY SHOULD BE DONE AT A HADRON THERAPY CENTER

G. Kraft, W. Kraft-Weyrather, G, Taucher-Scholz, M. Scholz

((Presented at the "2nd Symp. on Hadron Therapy", Cern,Geneva,Switzerland,Sept 12,1996)

Gesellschaft für Schwerionenforschung mbH
Planckstraße 1 • D-64291 Darmstadt • Germany
Postfach 11 05 52 • D-64220 Darmstadt • Germany

What Kind of Radiobiology should be done at a Hadron Therapy Center

Gerhard Kraft, Wilma Kraft-Weyrather, G. Taucher-Scholz and M. Scholz
Biophysik, GSI, Darmstadt

Introduction

Although therapy with heavy particles like neutrons, protons or heavier ions has now a rather long history of several decades [1], but there are more open questions than settled problems. This fact is really amazing because the use of the high LET particles, neutrons and heavy ions was strongly motivated by radiobiological arguments [2]. Presently, the use of protons with a better physical dose distribution is more widely accepted than neutrons or heavy ions where the expected high LET benefit could not be verified clinically. This demonstrates that predictions made on the basis of radiobiological experiments cannot be transferred directly from *in vitro* experiments to the therapy situation. In particular, it is not possible to transfer an average RBE value measured *in vitro* in an extended exposure field to the treatment situation. Therefore, in the following section the dependence of RBE on LET, dose and radiosensitivity will be summarized and compared to models. Basic experiments illustrating the RBE problem in a particle field will be described. The fundamentals of a recently developed track structure model will be given and calculations will be compared to experiments. Finally, a short outline of possible future developments for radiobiology will be presented.

Advantages of Hadrons in Therapy

Using hadrons can have the following advantages compared to conventional therapy: A better physical selectivity meaning an improved dose profile and a higher biological efficiency corresponding to greater killing in the tumor [3]. However, the various hadrons differ in their properties. In fig. 1 the depth-dose relationship of photons, neutrons, negative pions and ions are compared. Obviously, the neutrons have a similar dose distribution as the photons while charged particles are characterized by an inverse profile, i.e. an increase of dose with penetration depth. The inverse dose profile allows a greater dose in the target volume and consequently a better tumor control. Neutrons do not exhibit this advanced physical dose profile but differ in their relative biological efficiency (RBE) from photons. The higher RBE yields a better tumor control but also a greater complication rate of the healthy tissue because for neutrons the regions of high RBE cannot be restricted to the target volume alone. The

ultimate strategy for an advanced hadron therapy is to optimize both, physical and biological selectivity, which can be achieved using heavy ions [2]. But in this talk we will focus on the biological effects i.e. on the variation of the relative biological efficiency RBE alone.

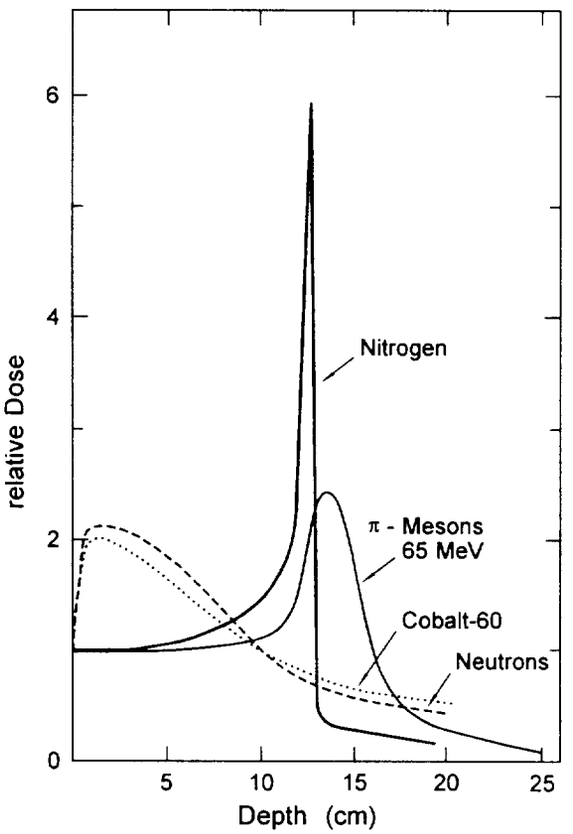

Figure 1: Comparison of the depth dose distribution of gamma rays, neutrons, pions and heavy ions. The charged particles exhibit an increase of dose with penetration depth while neutrons or gamma rays are characterized by an exponential decay for deeper penetration.

The Relative Biological Efficiency

The relative biological efficiency RBE is defined as the ratio of x-ray to particle doses necessary to produce the same biological effects [4]. This definition can be used in the case of survival curves as shown in fig. 2 but also for other dose effect curves as measured for intracellular effects (DNA breaks, chromosome aberration) or tissue effects or the survival of animals and men after exposure.

Usually, the x-ray dose effect curve for inactivation and other endpoints shows a large shoulder, in the terms of the mathematical description by a linear quadratic expression $\alpha D + \beta D^2$, a large β term. Particles of increasing LET are characterized by an increase of the α term and smaller values of β, finally reaching pure exponential survival curves ($\beta = 0$).

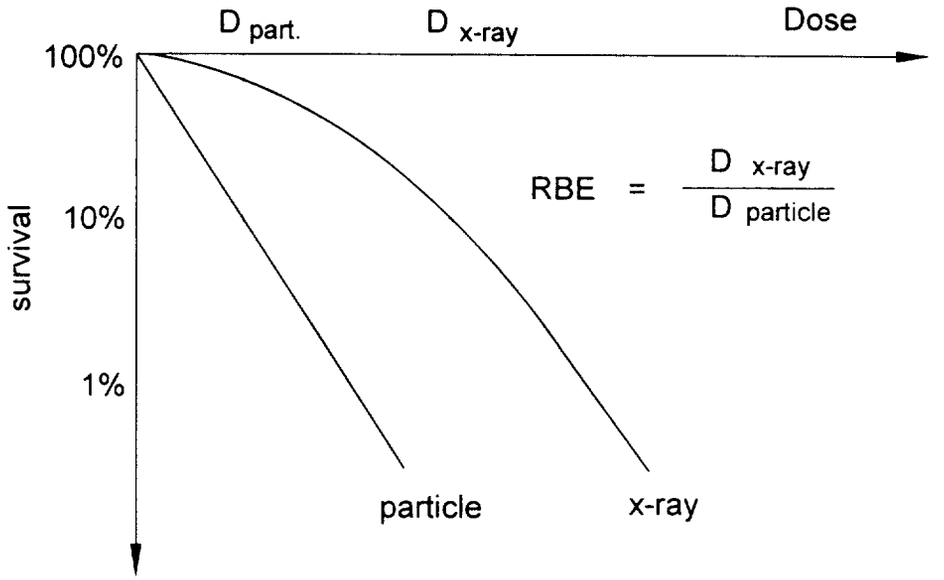

Figure 2: Using schematic survival curves for x-rays and particles the definition of the Relative Biological Efficiency is illustrated as the ratio of x-ray and particle dose producing the same biological effect.

According to this behavior RBE exhibits two major dependencies as function of LET. First, RBE increases with LET from one to a maximum value and decreases beyond this maximum to values smaller than one (fig.3). Frequently, the increase in RBE is interpreted as a higher production rate of locally correlated damage. In the maximum of the RBE an optimum of correlation should be reached where one particle traversal should be sufficient to kill a cell [5].

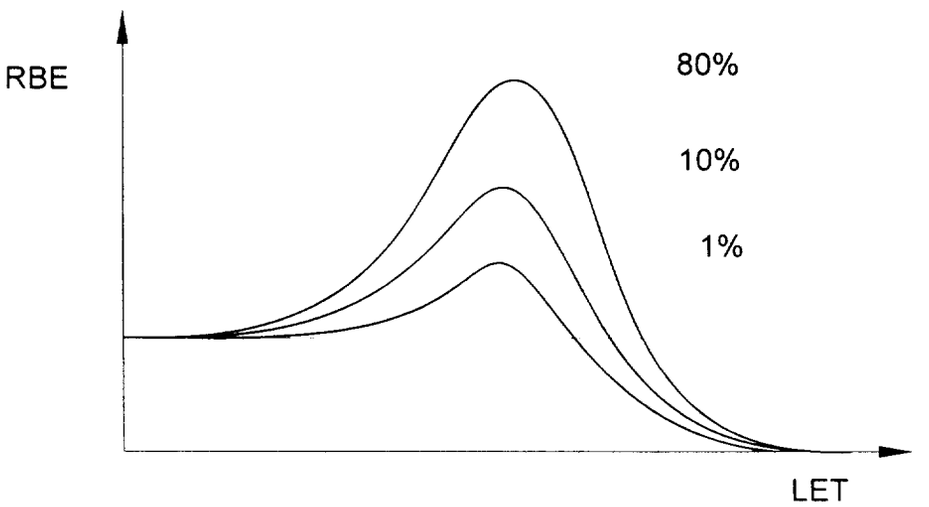

Figure 3: A schematic representation of RBE versus LET is given. Because of the shoulder of the x-ray dose effect curve, the RBE strongly depends on the effect level. For low doses the RBE is larger than for high doses.

Higher LET values are attributed to larger local damage, that cannot be expressed biologically because cell lethality has already been reached and the surplus of local energy deposition is wasted in form of saturation for which the military term "overkill" is used. [6].

The second finding is that for low doses corresponding to high survival levels the height of RBE maximum is larger than for low survival caused by high doses. This behavior originates from the shoulder of the x-ray survival curve at low doses. Particles mostly exhibit a pure exponential curve. Therefore, the difference between both is large at small doses. However, for extremely high doses both curves become parallel and the RBE reaches asymptotically one. The position of RBE maximum does not significantly depend on the survival level as long as the type of particle remains the same. However, the LET position changes if the atomic number is varied (fig.4]. For protons the RBE maximum is at 25 keV/μm, for He-ions at 100 keV/μm and for heavier ions at higher LET values but with lower absolute height.
Finally, if we study cells or tissues of different radiosensitivity we can find different RBE values using beams of the same quality. In general, it is found that RBE is greatest if the repair capacity is large i.e. the shoulder in the x-ray survival curve is large. For radiosensitive material the shoulder in the x-ray dose effect curve is reduced and the RBE maximum becomes smaller (fig. 5.) If the shoulder disappears, as it is the case for very sensitive cells, hardly any RBE maximum remains [7].

The shoulder in the x-ray survival curve is correlated with repair: Repair-proficient cells exhibit a large shoulder, repair-deficient cells have no shoulder. Correspondingly. RBE has a large maximum for repair-proficient cells and a small or no maximum for repair-deficient cells [8].

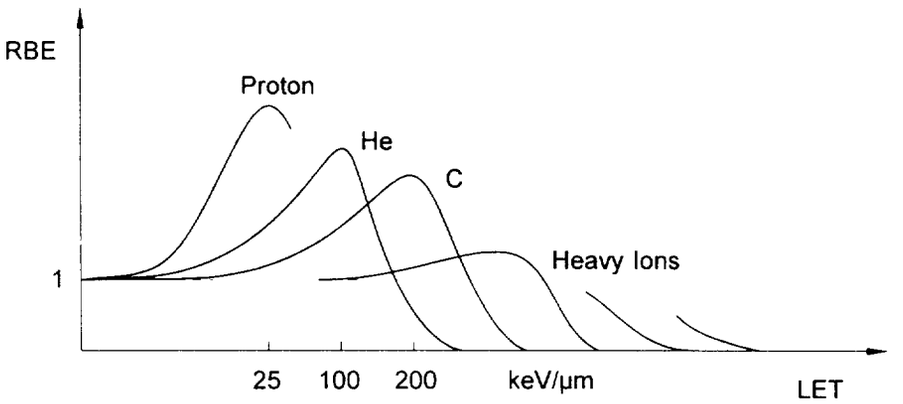

Figure 4: The RBE-LET relationship is given schematically for particles of different atomic numbers. For protons the RBE maximum is found at a LET value of 25 kev/μm, for He-ions at 100 keV, for carbon at 250 KeV/μm and for heavier ions at higher LET values.

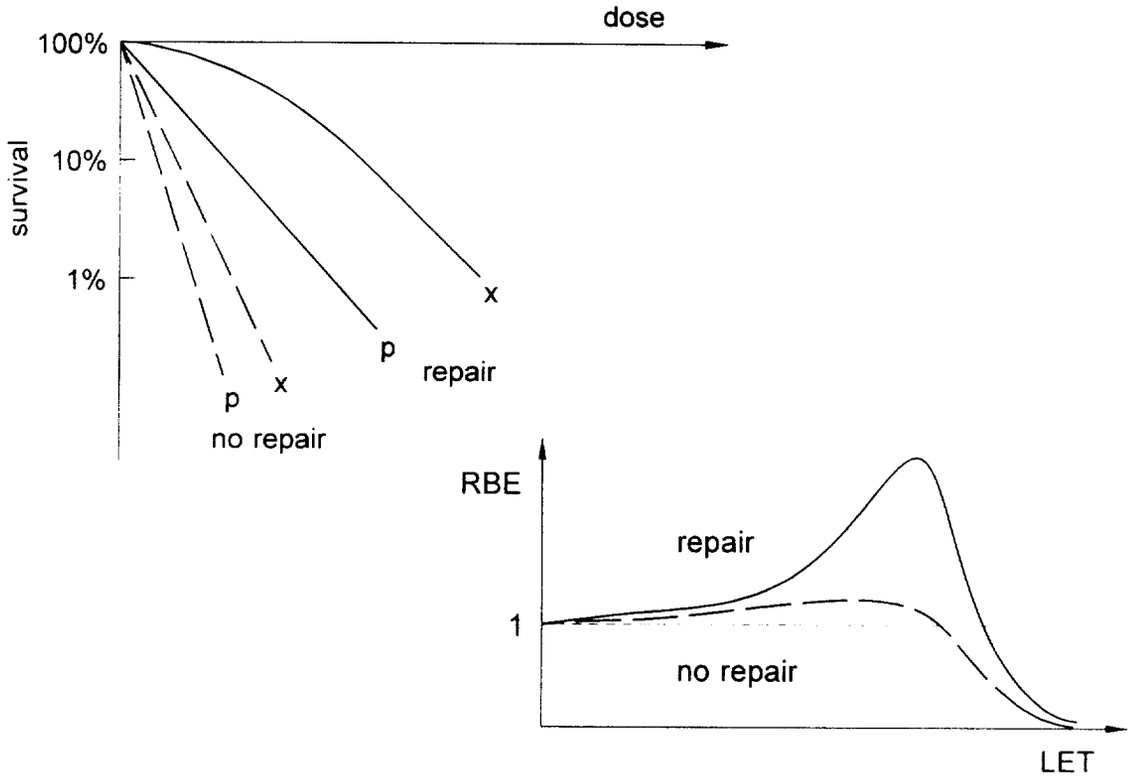

Figure 5: Cells and tissues of high repair capacity are characterized by a large shoulder in the dose effect curve that disappears for high LET exposure. Consequently a large RBE value is found while for repair-deficient cells the difference between x-ray and particle dose effect curve is smaller and consequently RBE is lower.

The LET Dependence of RBE

The common interpretation of the variation of the RBE with LET is very mechanistic. If the extension of the tracks is neglected the LET can be correlated to a local dose. Therefore, a higher LET is correlated to the induction of a larger amount of local damage [5]. This statement also seems to be true if we compare in a nanometer scale the DNA molecule with the pattern of ionization in particle tracks. In fig. 6 calculated proton and carbon tracks at 0.1, 1 and 10 MeV/u are compared to a schematically given DNA molecule [9]. For the protons of higher energy it is obviously possible to traverse a DNA molecule without producing any damage. Most frequently one electron is created and DNA damage originates from the action of this isolated electron as it is the case for sparsely ionizing radiation. At the lowest energy shown, ionisation events in the proton track become more close and the probability to induce two events in close proximity becomes much larger, in consequence, the probability to produce a lesion at the two opposing DNA strands i.e. a DNA double strand break is enhanced.

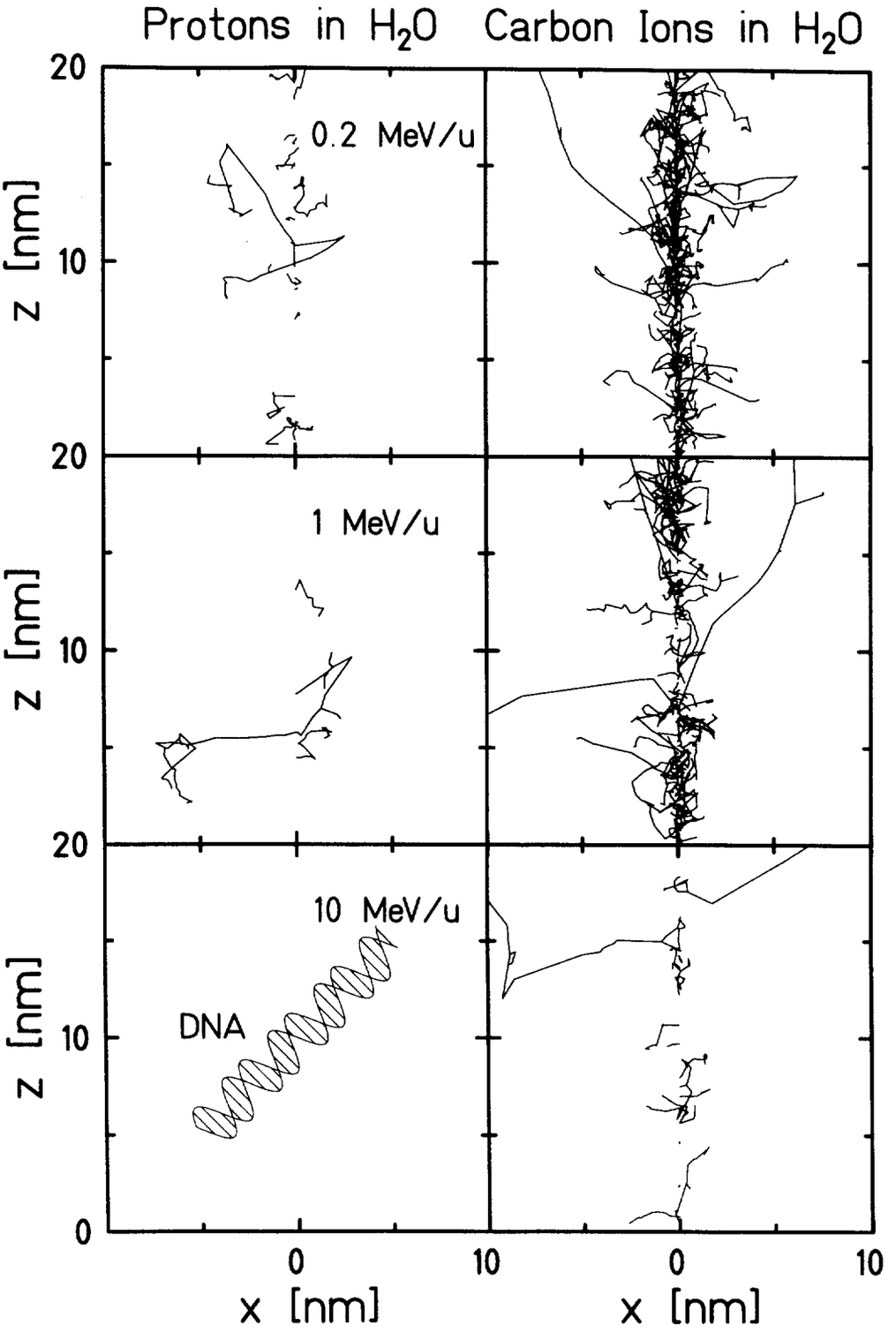

Figure 6: Calculated tracks of protons and carbon ions are compared with the dimensions of a schematic view of a DNA molecule. Evidently, the chance of multiple ionization events in the DNA molecule is much higher for carbon ions at low energy.

In the carbon track the production of correlated damage is drastically enhanced because of the much higher density of primary and secondary ionization events. Therefore, one expects a higher number of DSB that cuts the DNA into small fragments yielding a greater probability to produce cell death.

Using tools of modern molecular biology it is possible to test this assumption of a high fragmentation directly. In heavy ion experiments cells embedded in an agarose gel and were exposed to a carbon beam that has its Bragg maximum in the middle of the gel. After exposure the cells are lysed and DNA fragments extracted while undamaged DNA is retained in the plug. Using a proper calibration the number of DSB can be calculated and compared to the local dose i.e. the Bragg curve (fig. 7).

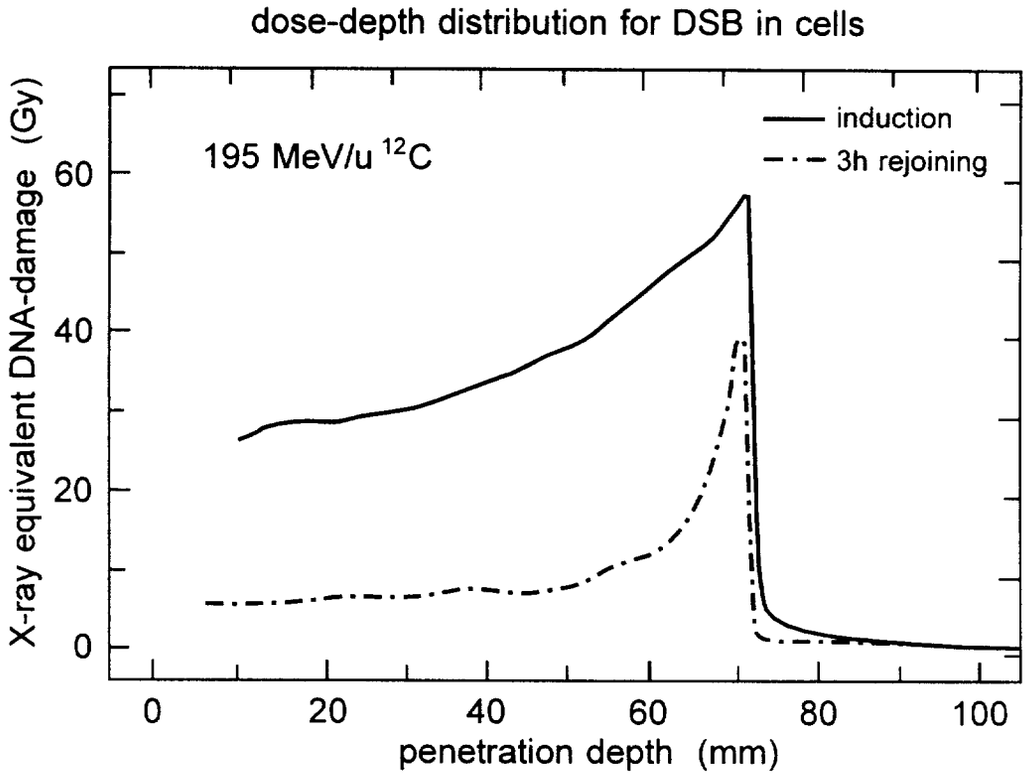

Figure 7: The amount of double strand breaks immediately after exposure to 200 MeV/carbon ion and after an additional incubation time of 3 hours for DNA repair is shown as function of penetration depth. In the entrance channel most of the breaks are repaired.

In this experiment more breaks are found towards the end of the range, but the ratio between plateau and "biological" Bragg maximum is smaller than 1:2, while the physical Bragg curve has a ratio of 1:6. These measurements very strongly suggest that the high RBE in the Bragg maximum for cell killing cannot be attributed to an enhanced production rate of double strand breaks only [11]. The same result has also been found in track segment experiments where the

increase in RBE with larger LET values is not paralleled by the corresponding DSB induction rate [12].

However, judging such an interpretation one has to envisage that the resolution of DSB - detection assay is rather poor. Small fragments of a few tens or a few hundreds of base pairs are not detected. Therefore, clusters of DSB in close proximity of less than approximately 100 base pairs will not be detected. But the production of DSB clusters is exactly the effect that is expected for heavy particle irradiation. In order to verify the production of multiple damaged sites indirect methods have to be used.

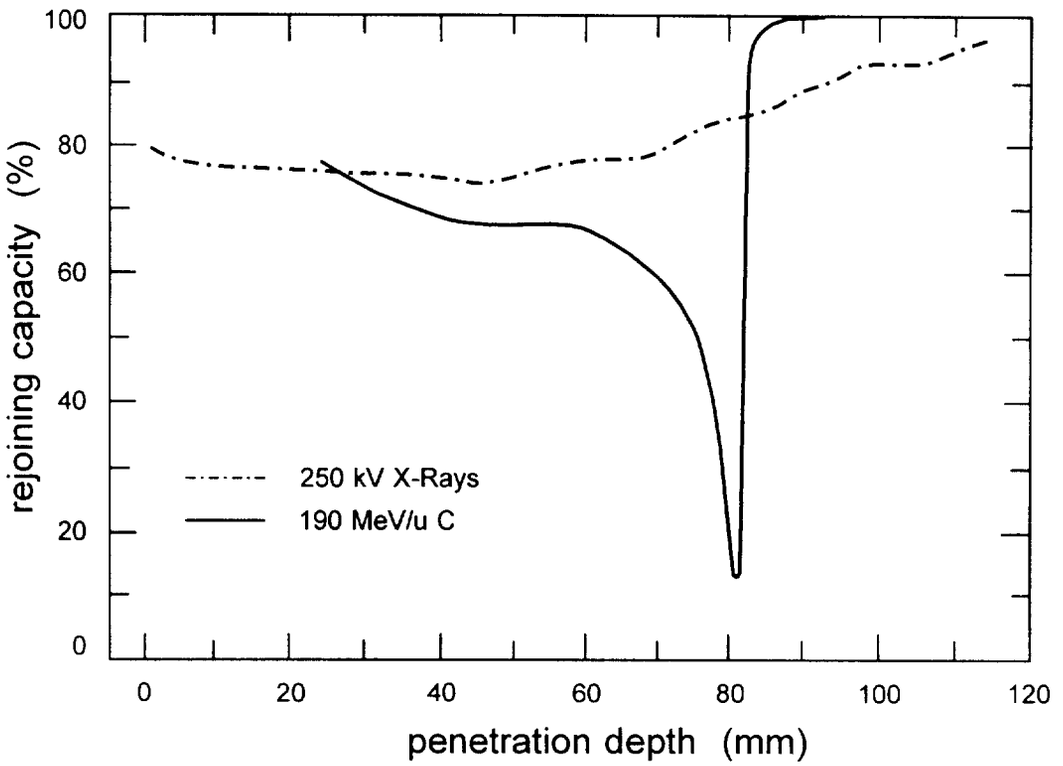

Figure 8: Comparison of the rejoining after x-ray and particle exposure as function of penetration. For carbon ions and x-rays approx. 80% of breaks are rejoined in the entrance while in the Bragg maximum the amount of irrepairable damage strongly increases only for the particles.

The track segment experiment as well as the "mega-plug" experiment exhibit a very different result when after a repair interval the number of residual breaks i.e. non-repaired or non-rejoined double strand breaks is measured again. Then the region of the elevated LET in the Bragg maximum shows a large amount of non-rejoinable breaks while breaks in the plateau are rejoined to a large extent. The ratio between plateau and Bragg maximum becomes comparable to the energy deposition but it should be noted that the number of non-rejoinable breaks is not exceeding the level of physical dose deposition. For cell killing larger effects

than those proportional to dose are found. This is due to the following effect: In the experiment it is not distinguished between genetically correct or incorrect repair, the observed higher killing efficiency is probably due to the induction of sites with multiple damages that have a lower probability of correct repair. For the carbon beam as shown in fig. 8 about 80% of the initial lesions are rejoined in the Bragg maximum. For heavier ions in the entrance channel more irrepairable lesions are produced. For lighter ions like protons the entrance channel stays the same but the efficiency in the Bragg maximum is reduced.

However, in all cases the correlation between cell survival and double strand breaks is more likely to be given by the amount of irrepairable lesions and not by the pure induction rate of damage. This optimum ratio of repairability between entrance and target volume is a major argument for the use of carbon in therapy.

Cellular Inactivation Measurements

The molecular findings of an enhanced RBE in the Bragg maximum is paralleled by the measurements of cell inactivation as shown for instance in fig. 9. CHO-cells have been exposed in a waterphantom to a 270 MeV/u carbon beam and the RBE was assessed for particle fluences of 2 or 5 x 10^6 particles/cm^2 by comparing the expected survival using x-rays with the actually measured inactivation values. In accordance with the previous statement the RBE is smaller for higher particle fluences and doses. However, for both doses the functional dependence of the RBE is paralleled by the molecular measurements described in the DNA experiment above. In addition, the decrease of the RBE in the mid of the plateau region, that is due to beam fragmentation, nicely shows up in the survival measurement and in the calculated RBE. Fragments created by nuclear reactions have lower atomic numbers [13] and therefore produce a lower biological effect.

In the case of the treatment of an extended target volume like a tumor superpositions of Bragg curves have to be used in order to fill a complete target volume [14] (fig.10). In these extended Bragg curves the RBE has to be assessed with regard to the mixture of particles of different energies and of different atomic numbers due to the beam fragmentation. Because RBE is related to the dose in a non linear proportion, it is not possible to determine experimentally or theoretically a "biological effective" Bragg curve and superimpose those biological Bragg curves. In an extended Bragg maximum the RBE critically depends on the

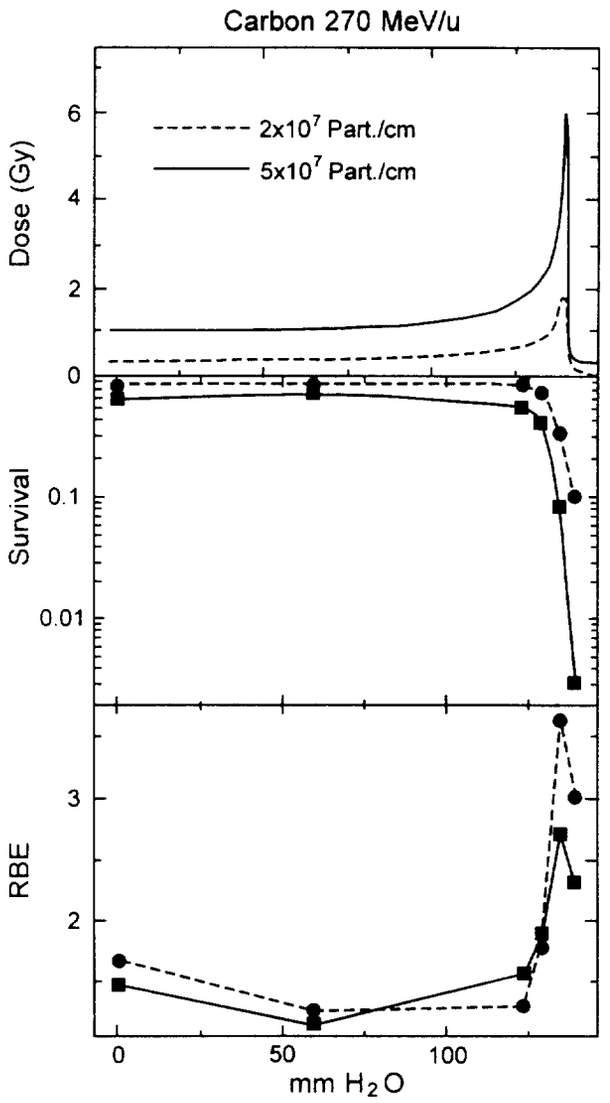

Figure 9:

In the upper panel the energy deposition due to the exposure to 2 and 5 x 10^7 carbon ions per cm^2 is compared to the corresponding cell survival (mid panel) and RBE (lower panel) as function of penetration depth.

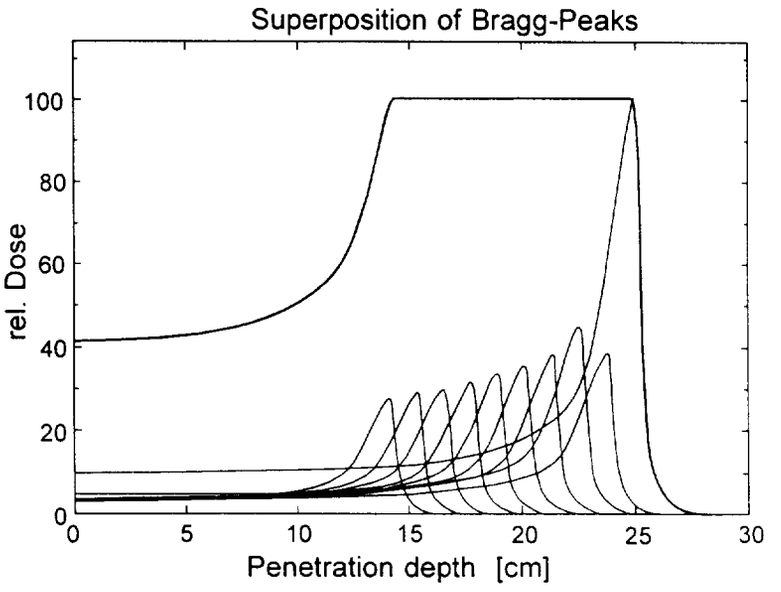

Figure 10:

For the exposure of an extended target volume Bragg curves of different energies were to be superimposed. In such an "extended" Bragg volume the dose in each point originates from particles of different energies.

local composition of the beam in energy, atomic number and intensity. This is illustrated in fig. 11 where extended Bragg curves of different physical dose shapes are used to determine survival and RBE. Although it was the goal of these experiments to achieve a flat top of cellsurvival over the target volume, the increase in RBE towards the distal end of the extended Bragg curve was slightly underestimated for high doses [16].

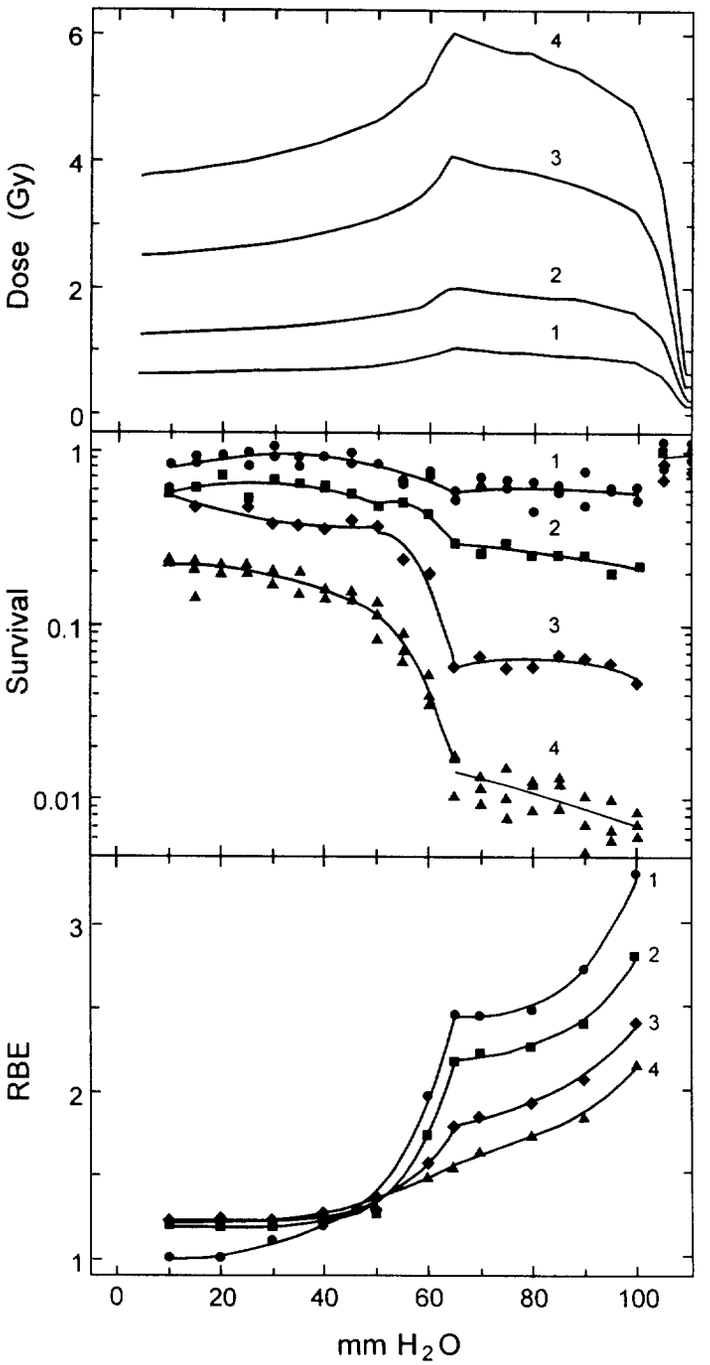

Figure 11: For the different particle fluences dose, survival and RBE are compared as function of penetration.

These measurements reveal two important facts: First, at therapeutically realistic doses of 2 Gy in the tumor, the RBE in the target volume is between 2 and 2.5 i.e. very close to the neutron RBE. In the plateau region the RBE stays close to photon values, reaching 1.3 to 1.5. Ions heavier than carbon produce slightly higher RBEs in the target but much higher RBE values in the entrance channel [17] Therefore, the biological gain factor becomes smaller. In consequence, a heavy ion beam of carbon ions represents the best combination of high efficiency in the target volume and tissue sparing in the entrance channel. Secondly, these measurements demonstrated that in the case of tumor conform treatment large variations of RBE are to be expected. For oddly shaped volumes these variations of the local RBE can only be predicted using a realistic biological model for the RBE. Such a model must be able to reproduce not only single survival curves of track segment experiments but also the response in mixed fields as created in an extended Bragg maximum or in neutron irradiation.

Theoretical Approaches

Radiobiological models can be classified in either physics or biology oriented. The physics oriented models try to attribute in a determinative way the final fate of the biological lesion to the structures of the physical energy deposition. Physics models do not include any variability of the biological response like repair. Biology oriented models are mainly based on repair, non- or misrepair with minor attention paid to the primary structures of the physical event. It is a very controversial point of particle radiobiology that from all models the track structure model yields the best agreement with the experimental reality but does not include repair or detailed physical parameters, while biology oriented models as well as microdosimetry or target theory fail to predict experiments [18].

For instance, the track structure models in their original form [6] predict the formation of individual σ-LET hooks for each atomic number. In the model calculation the radial dose distribution in $\frac{1}{r^2}$ form is integrated over all distances corresponding to the target area and survival is calculated by comparing the particle dose to the x-ray dose.
In the thin down region towards the end of the track higher doses are transferred to the cell nucleus as target than necessary for inactivation - yielding the above mentioned overkill effect. Because radial doses are integrated over the complete track diameter, the saturation depends on the track structures and the hooks are separated in order of increasing atomic number as confirmed by the experiment.

In a more sophisticated version of the track structure model [19] two different types of inactivation are assumed - ion kill and gamma kill. In addition, there are more parameters that have to be fitted in order to achieve a good overall agreement with the experiments.

Recently, an attempt has been made to include repair and the dependence of biological effects on the local dose inside the track [20, 21]. In this refined model the particle track is divided into radial zones of nearly equal dose and the biological effect is calculated for these local doses using the complete x-ray effect curve. Then, instead of dose integration the biological effect i.e. the number of lethal lesions is integrated over the target volume. Because the biological effect is taken from all points of the shouldered x-ray effect curve repair is as much included here as it is in the x-ray curve.

The essential parameters of this calculation are the x-ray dose effect curve, the average geometrical size of the nuclear target and the radial dose of the particle tracks. With this information, the complete survival curves for particles can be calculated. Because it is based on the x-ray dose effect curve, the track structure model in its improved form represents rather a recipe to include the inhomgeneous dose distribution caused by the particle tracks than a basic understanding of the action of ionizing radiation in general.

But within this limitation the model is able to predict the biological response to particle radiation with an unexpected accuracy. This is even true for neutrons that produce a mixed field of particles or the superposition of Bragg and plateau ions as it is found in the extended target volumes [15].

Comparison of Measured and Calculated Data

If calculations are to be used for therapy planning one has to assure that the calculated results are in good agreement with the biological reality. Therefore, sets of experiments have to be used where under well defined conditions the inner consistency of the data can be verified. Obviously, the first tests are verifications of survival curves with different ions and different energies. In fig. 12 a set of survival curves of carbon ions at different energies is shown. In order to obtain a realistic comparison with the therapeutical scenario, the ions are decelerated in water and produce the same amount of nuclear fragments as they do in the patient. The influence of these fragments is evident, showing the 195 MeV/u survival curve at 6 cm depth above the curve of the initial energy. Although the LET of the primary carbon ions increases, the biological effect decreases initially because of the production of lighter fragments that have a lower biological efficiency [13] Closer to the Bragg maximum the increase in LET

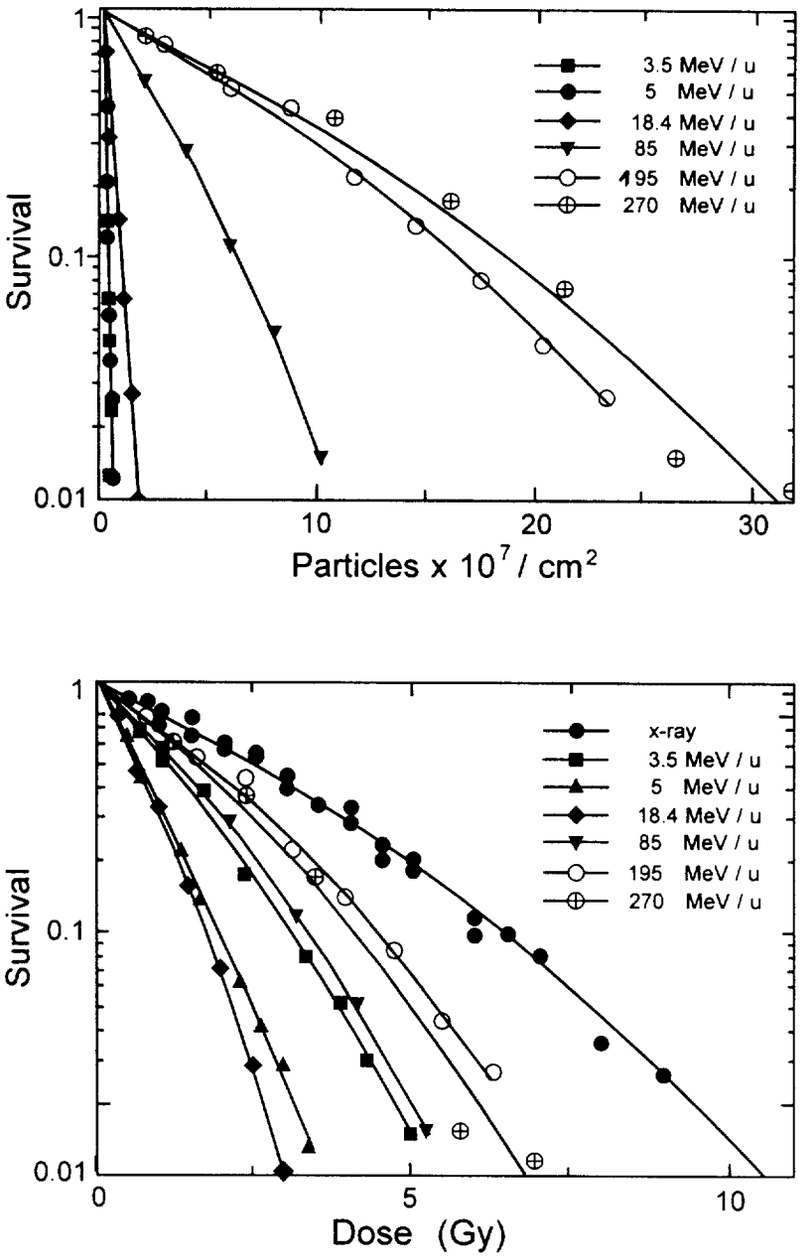

Figure 12: Survival curves of CHO cells exposed to a 270 MeV/u carbon beam at different penetration depth corresponding to different energies. In the top panel the data are given as function of the particle fluence, at the bottom panel as function of dose, together with a x-ray dose effect curve. With decreasing energy the carbon ion become more effective. The influence of the beam fragmentation interchanges the 270 and 195 MeV/u curve.

overcompensates the influence of nuclear fragmentation. There, the inactivation efficiency increases again. The calculated data are based on measured fragmentation cross sections [22 and ref. given therein]. The agreement between calculation and experiment is remarkable.

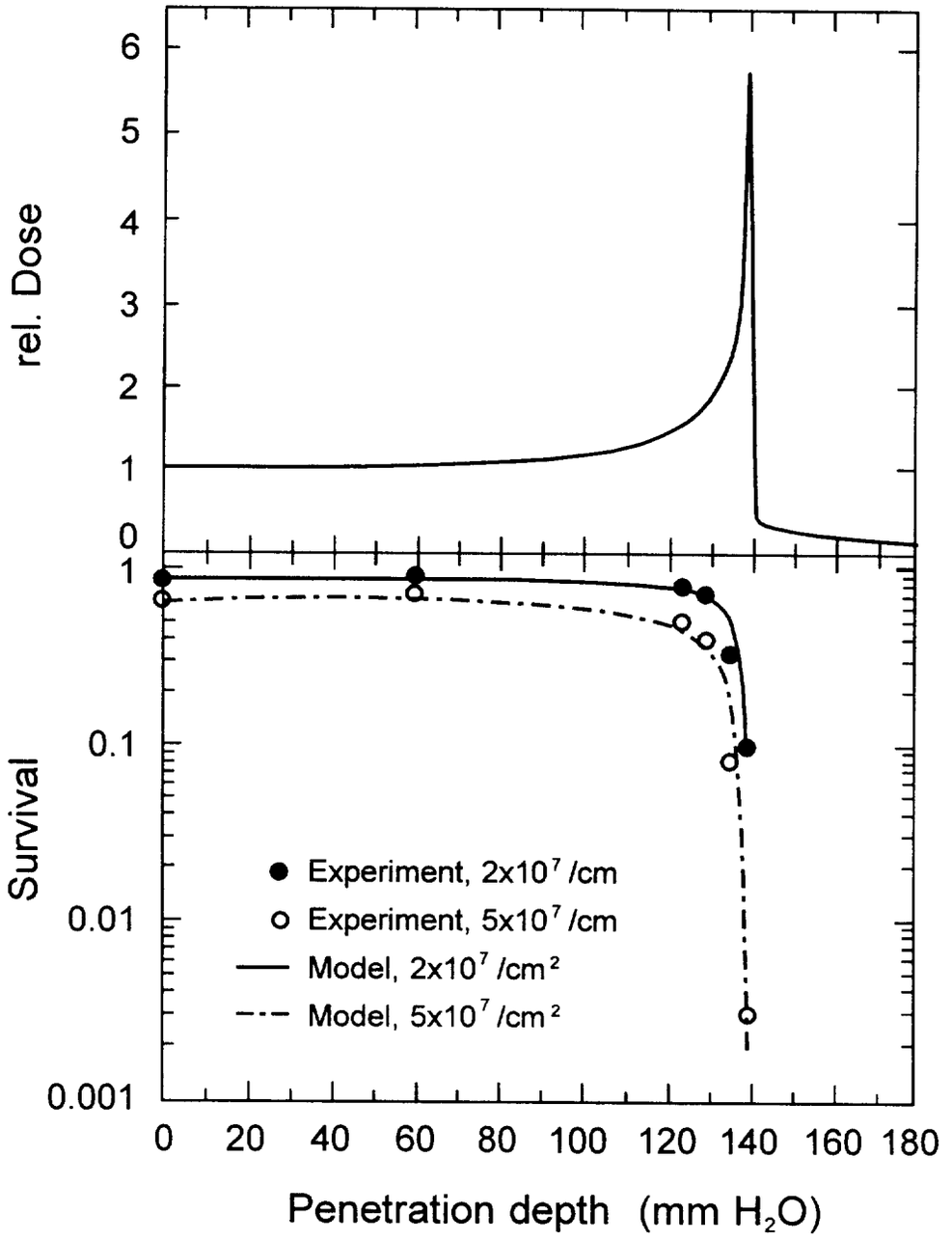

Figure 13: The same data as given in fig. 11 are shown together with a calculation according to the track structure model described in the text.

If it is possible to calculate the complete survival curve at any given depth, the inactivation by a beam of a given particle number as function of penetration depth can be calculated too (fig. 13).

The next step of verification is the comparison of calculated and measured survival in an extended Bragg peak as it will be used in therapy later on. For this purpose a scenario for the irradiation of a target volume with a diameter of 4 cm in the middle of the head is shown as would correspond to the situation of the irradiation of a brain tumor. Two extended Bragg

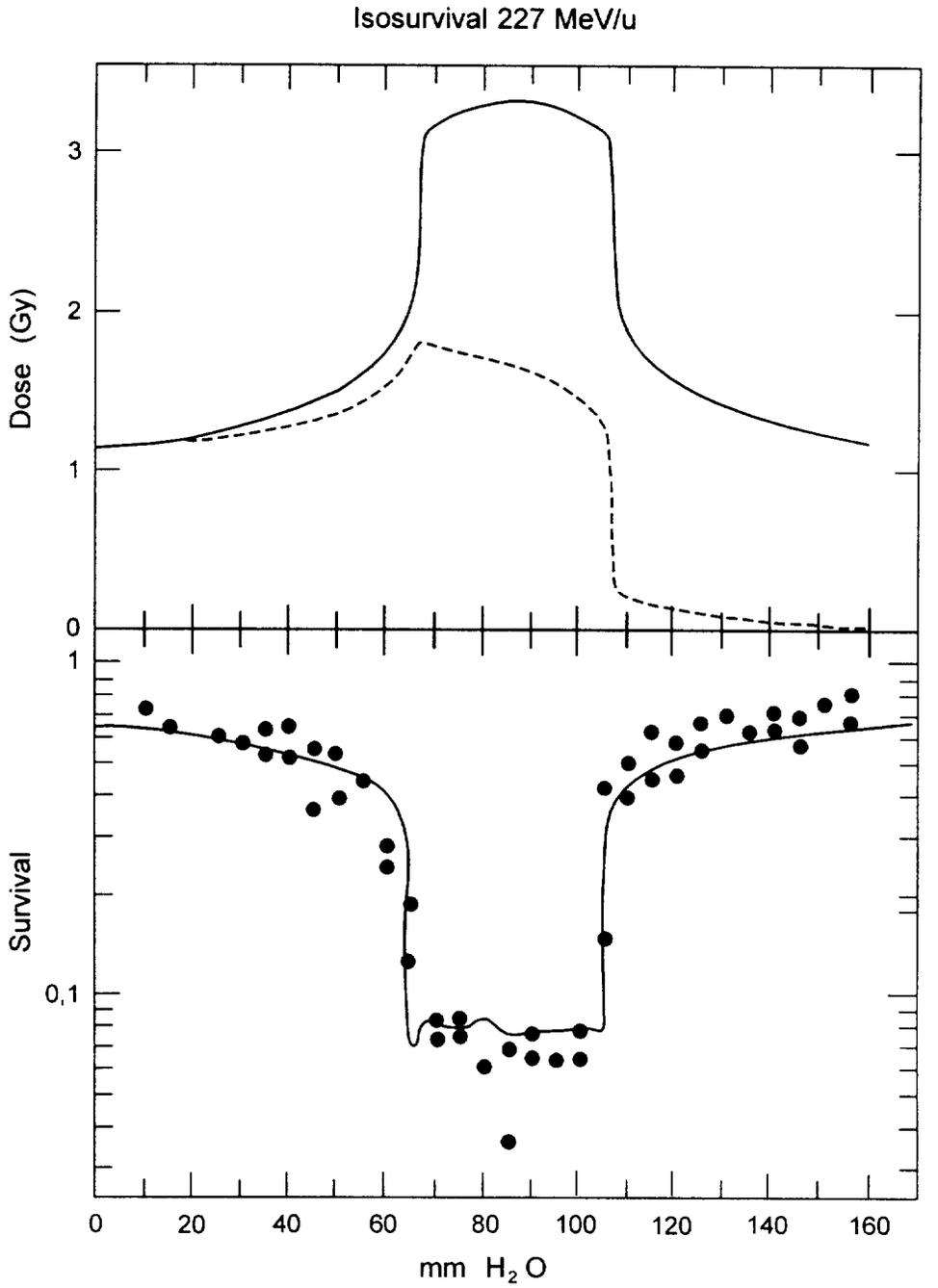

Figure 14: In a phantom simulation CHO-cells were exposed to an extended Bragg peak from two opposite sides. The measured cell survival (points) and the calculated data (line) show in excellent agreement the high efficiency in the simulated target volume.

maxima were applied from opposite sides and the survival was measured with the same technique as used before. The results shown in fig. 14 again show excellent agreement with the theoretical curve.

The new model enables us to calculate the particle effect on the basis of the x-ray response curve and track structure. In order to test the limitations of this approach *in vivo* measurements

with tissues have to be carried out. Corresponding experiments were performed with mice, rats and minipigs. Results of the minipig experiment will be presented [23]. This comparison implies the transition from *in vitro* data to *in vivo* data.

From x-ray fractionation measurements, values α and β of a hypothetical survival curve were determined and, assuming reasonable target sizes, the effects of fractionated particle irradiation was calculated. Details of this kind of calculations are given in the ref. [15]. In fig. 15 the effects on pig skin after 5 daily fractions of x-rays are compared to carbon exposure. It should be noted that the equivalent particle dose is given in Gray equivalent, i.e. in physical dose multiplied by the RBE calculated before. Again, the biological effect of particles and x-rays are in excellent agreement.

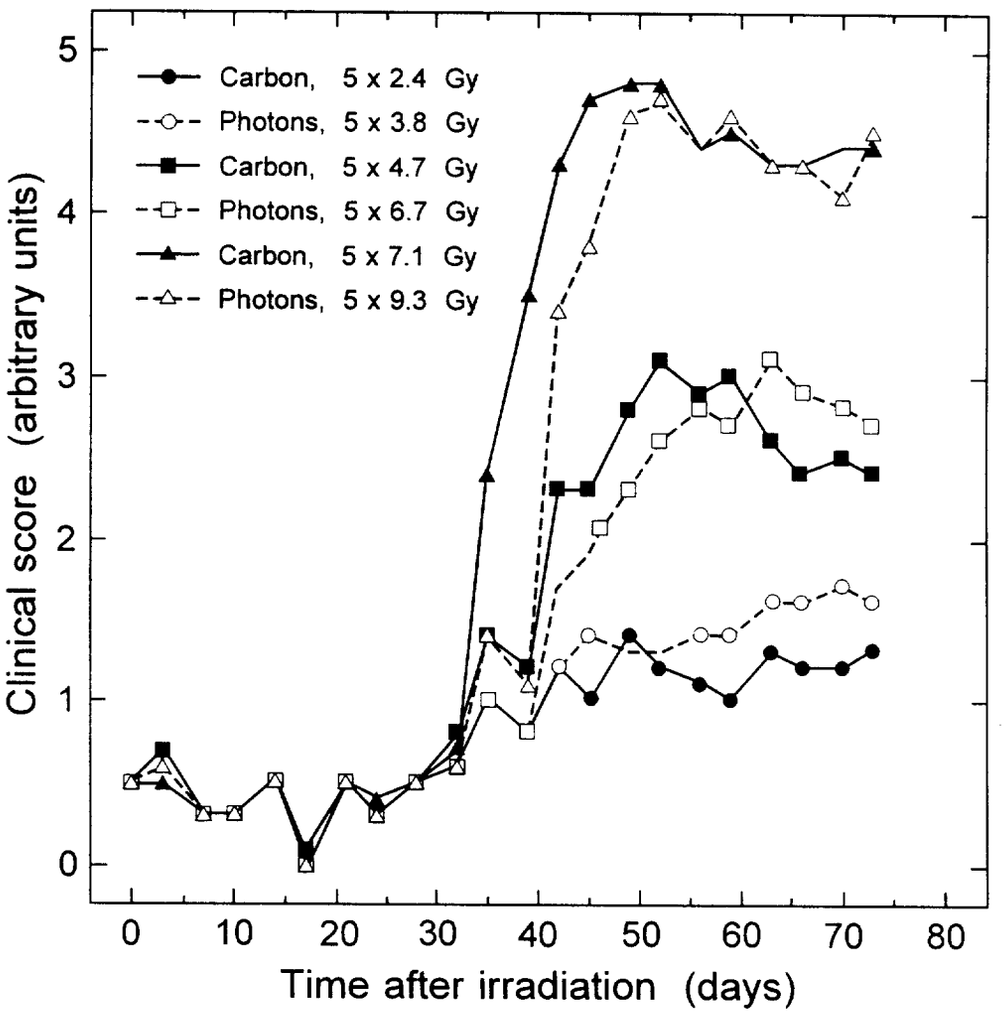

Figure 15: Acute responses of pig skin to the exposure to ^{12}C-ions and 200 kv x-rays are compared for three levels. In the carbon doses calculated RBE values are used to achieve the same biological response.

Presently, a large number of these experiments, comparing the measured particle effects with those calculated on the basis of x-ray dose effect curves and track structure, are performed. In these experiments no major discrepancy could be detected. This very much confirms the validity of the calculations used for *in vitro* experiments and also for response of tissues after fractionated exposure.

Future Radiobiology for Hadron Therapy

The work accomplished up to now demands the following research in the next future: First, the success of the unified track structure model deserves a broad affirmation of its fundamental basis. This is true for the mathematical approaches as well as for the molecular basis of the very heuristic approach. Secondly, the progress achieved with the unified track structure model has to be integrated into treatment planning. This is not a sequential step after the exploration of the molecular basis - this has to be and is done right now [24]. There was very successful chemistry long before the nature of the chemical bonds was understood by quantum mechanical explanation. Therefore, the application of experimentally confirmed models can be used in treatment planning before its foundations are completely understood. The main task in treatment planning is the creation of a local field of RBE values over the total exposed tissues, i.e. tumor and healthy tissue that can be used to maximize the effect in the tumor but also optimize the tissue sparing.

Finally, the attempt should be made to develop predictive assays for the particle treatment. This is the most difficult task, because such assays do not exist for x-ray treatment either. But it would be a major step forward, if we could select patients according to certain criteria helping us decide whether they should undergo particle treatment at all and if so of what type. These predictive assays for particles are not necessarily coupled to similar assays for x-ray exposure. But it is very likely that x-ray assays would be a very good starting point for particle therapy.

In summary: radiobiology for hadron therapy has the tasks of a fundamental research, finding and describing the difference in particle action, developing theoretical methods, that can be implemented into treatment planning and producing predictive assays that help in the patient selection.

ACKNOWLEDGEMENTS

We express our thanks to the colleagues of the biophysic groups at GSI for many helpful discussions and for making experimental data available, especially to Michael Krämer for placing figure 6 to our disposal. We thank Kirsten Langbein and Belinda Bathelt, who prepared the manuscript.

References

[1] Raju M.R.: Heavy Particle Radiotherapy: Academic Press, New York, 1980

[2] Wambersie A., The Future of High-Let Radiation in Cancer Therapy, in: Chauvel P. and Wambersie A., Eulima Workshop on the Potential Value of Light Ion Beam Therapy, Publication No. EUR 12165, Commission of the European Community, Brussels, 1989

[3] Kraft G., The Radiobiological and Physical Basis for Radiotherapy with Protons and Heavier Ions, in:Strahlentherapie und Onkologie, 166 (1990), 10 - 13

[4] The Quality Factor in Radiation Protection, ICRU Report 40 (1986)

[5] Hall E.: Radiobiology for the Radiologist: J.B. Lippincott Company, Philadelphia, 1994, fourth Edition

[6] Butts, J.J., R. Katz (1967), Theory of RBE for Heavy Ion Bombardement of Dry Enzymes and Viruses, Radiation Research, 30, 855-871

[7] Blakely E.A. et al., In Vitro Biophysics: Cellular and Molecular Studies, Annual Report of the Lawrence Berkeley Laboratory 1987, Biology & Medicine Division, University of California, 59 - 63

[8] Lett J.T., Cox A.B., Story M.D., Ehmann U.K. and Blakely E.A., Responses of Synchronous L5178Y S/S Cells to Heavy Ions and their Significance for Radiobiological Theory, Proc. R. Soc., 1989, B 237, 27 - 42

[9] Kraft G., Taucher-Scholz G. and Heilmann J., LET-Effects in DNA, in: Fuciarelli A.F. and Zimbrick J.D., Radiation Damage in DNA, Battelle Press, 1995, 203 - 214

[10] Heilmann J., Taucher-Scholz M., Kraft. G, Analysis of Native Cellular DNA after Heavy Ion Irradiation: DNA Double Strand Breaks in CHO-KI Cells, Radiation Damage in DNA, Int. J. Radiation Oncology Biol. Phys., 1996, Vol. 34, 599 - 608

[11] Kraft G., Radiobiology of Heavy Charged Particles, 1996 to be published in Physica Medica

[12] Taucher-Scholz G., Heilmann J. and Kraft G., Influence of Radiation Quality on Strand Breaks in Viral and Cellular DNA, in: Hagen U., Harder D., Jung H. and Streffer C., Radiation Research 1895 - 1995, Congress Proceedings, Vol. 2, Würzburg

[13] Schall I., Schardt D., Geissel H., Irnich H., Kankeleit E., Kraft G., Meagel A., Mohar M.F., Münzenberg G., Nickel F., Scheidenberger C. and Schab W., Charge-Changing Nuclear Reactions of Relativistic Light Ion Beams ($5 \leq Z \leq 10$) Passing through Thick Absorbers, Nuclear Instruments and Methods in Physics Research B 117 (1996), 221 - 234

[14] Haberer Th., Becher W., Schardt D. and Kraft G., Magnetic Scanning System for Heavy Ion Therapy, Nuclear Instruments and Methods in Physics Research A330 (1993) 296 - 305

[15] Scholz M., Calculation of RBE for Normal Tissue Complications Based on Charged Particle Track Structure, Bull Cancer/Radiother. Elsevier, Paris, 1996, 83 (Suppl. 1), 50-54

[16] Fournier C., Kraft G., Kraft-Weyrather W., Ritter S., Scholz M., Müller-Klieser W., Wachsmuth I., Zukowski D., Jüling-Pohlit L., Schopohl B., Alheit H., Enghardt W., Geipel C., Geyer P., Henzel P., Herrmann T., Kumpf R., Röthig H., Sobiella M., Weise R. and Zacharias T., Radiobiology Related to Heavy Ion Therapy, in: GSI Scientific Report 1995, Darmstadt, 139 - 146

[17] Blakely, E. A., C. A. Tobias, F. Q. H. Ngo and S. B. Curtis, Physical and Cellular Radiobiological Properties of Heavy Ions in Relation to Cancer Therapy Applications, Biological and Medical Research with Accelerated Heavy Ions at the Bevalac 1977-1980, Berkeley, 1980, 73-86

[18] Kraft G., Scholz M. and Taucher-Scholz G., Physics of Particle Tracks and Radiation Damage to Chromatin, to be published in Adv. in Space Res.

[19] Katz R. et al., Inactivation of Cells by Heavy Ion Bombardment, Radiat. Res. 47, (1971) 402-425

[20] Scholz M. Kraft G., Calculation of Heavy Ion Inactivation Probabilities Based on Track Structure, X-ray Sensitivity and Target Size, Radiat. Prot. Dosimetry, (1994) Vol. 52, Nos 1-4, 29-33

[21] Scholz M., Kraft G., Track Structure and the Calculation of Biological Effects of Heavy Charged Particles, Adv. Space Res., (1996) Vol. 18, No. 1/2, 5-14

[22] Schardt D. et al., This report

[23] Zacharias T., Dörr W., Enghardt W., Haberer Th., Krämer M., Kumpf R., Röthing H., Scholz M., Weber U., Kraft G. and Herrmann Th., Acute Response of Pig Skin to Irradiation with ^{12}C-ions or 200 kV/x-rays, submitted to: Physics in Medicine & Biology

[24] Krämer M. et al., This report